Construction and Building Materials 426 (2024) 136151

Contents lists available at ScienceDirect

Construction and Building Materials

journal homepage: www.elsevier.com/locate/conbuildmat

Statistical assessment of the factors influencing fly ash reactivity

Steffen Overmann[a,*], Lia Weiler[a,b], Johannes Haufe[a,c], Anya Vollpracht[a], Thomas Matschei[a]

[a] Institute of Building Materials Research, RWTH Aachen University, Schinkelstraße 3, Aachen 52062, Germany
[b] Stadtreinigung Hamburg AöR, Bullerdeich 19, Hamburg 20537, Germany
[c] ZERTplus Überwachungsgesellschaft mbH, Mühlenweg 11, Bitterfeld-Wolfen 06749, Germany

ARTICLE INFO

Keywords:
Calorimetry
R^3 test
Reaction
Particle Size Distribution
X-Ray Diffraction
Fly Ash

ABSTRACT

Siliceous fly ash is a pozzolanic supplementary cementitious material often used in cement and concrete production. The influence of the chemical, mineralogical and physical properties of 75 siliceous fly ashes on their reactivity was examined in this study. The reactivity was analyzed by relative mortar compressive strength and a rapid screening test (a version of the R^3 test). A statistical data analysis was carried out to evaluate the factors influencing the reactivity of the ash. The screening test was found to be able to predict the reactivity within short periods of time, while the relative strength is not a good measure for reactivity. It was also found that the TiO_2 and chloride content of the fly ash can serve as an indicator for its reactivity.

1. Introduction

The use of pozzolanic and latent hydraulic supplementary cementitious materials (SCMs) as main components in cement has been increasing within the last decades. In addition, materials such as fly ash, silica fume and ground granulated blast furnace slag are directly used as separate raw materials in concrete production. However, the reactivity and therefore the contribution to strength development during hydration varies considerably, not just between different materials, but also within one group of SCMs [1–3]. The accurate determination of the actual contribution of a SCM is essential to predict the strength development of concrete.

Internationally, a variety of test procedures exists to determine the reactivity of SCMs indirectly, e.g. by testing the compressive strength of a mortar containing a mixture of cement and SCM. Requirements and testing procedures for fly ashes are documented in the American standards ASTM C618 / ASTM C311 and the European standards EN 450–1 / EN 196–1. Unfortunately, the results of these tests depend on the properties of the specific reference cement; a phenomenon already stated by Sybertz [4].

Therefore, a testing procedure is needed, that can predict the reactivity of a SCM in the hydration process independently of the cement within a short time. The RILEM TC 267-TRM has tested different methods to determine the reactivity of SCMs [5]. The test methods considered in the work of the committee were the Chapelle Test [6], the Frattini Test (EN 196–5), the determination of reactive silica (EN 196–2), the Indian test method for pozzolanic materials (IS 1727–1967) and the so-called R^3 test method (R^3 for Rapid, Reliable and Relevant) which is focusing on the heat produced or the water bound during reaction in an artificial cement like environment [7]. The latter seems to be the most promising test method and was verified for a wide range of materials by Londono-Zuluaga et al. [8]. The R^3 test, which has first been published by Snellings et al. [3], was developed to obtain data concerning the reactivity of a SCM independent from its use in a blended cement. Therefore, a chemical environment like the one present during hydration is simulated using analytical grade chemicals such as portlandite, sulfates and alkalis. A relatively high water to solid ratio ensures that enough reaction medium is present, the elevated temperature of 40 °C, at which the tests are performed, results in a slight acceleration of the reactions without changing the reactivity mechanisms significantly.

As this study started in 2016, the primary test version according to [3] was performed for all relevant investigations. Meanwhile the test was optimized [7,9] and published in 2020 as ASTM C1897 – 20 [10].

The reactivity of fly ash glass depends strongly on the alkalinity of the pore solution of the cement paste. Additionally, the scientific community discusses several other physical and chemical properties of fly ashes that may impact the reactivity more or less intensely. Pietersen et al. already gave an overview on possible factors in 1989: the particle size distribution, the glass content and the glass chemistry are discussed as being the most influencing factors [11]. These factors and the reactive silicon content are subject to more recent studies as well [12–16].

---

* Corresponding author.
E-mail address: overmann@ibac.rwth-aachen.de (S. Overmann).

https://doi.org/10.1016/j.conbuildmat.2024.136151
Received 31 July 2023; Received in revised form 22 November 2023; Accepted 4 April 2024

However, the factors influencing the reactivity are still not understood in detail. Therefore, in this study numerous fly ashes were investigated with a multitude of methods in order to understand these factors more in-depth.

2. Materials and methods

2.1. Overview of the tested fly ashes

Representative samples of 75 different hard coal fly ashes from 15 different plants (13 plants from Germany, 1 from Mauritius, 1 from France) have been collected over the course of seven years between 2015 and 2021 mainly as part of external quality control, but also from research projects. An overview of the sample numbers from the different plants is given in Table 1. Detailed information on the individual samples are given in the electronic supplement.

2.2. Characterization methods

2.2.1. Chemical analysis

For the chemical analysis the fly ash samples were ground to a maximum grain size of 125 μm and dried at 105 ± 5 °C to constant mass. The loss on ignition was determined according to EN 196–2 on samples of 1.00 ± 0.05 g at 950 °C in a muffle furnace. To analyze the carbon and sulfate contents, a carbon/sulfur analyzer Eltra CS-2000 was used. By double determination, 0.150 ± 0.001 g of the fly ash sample were weighed in an annealed ceramic crucible and covered with 0.7 g iron granules and 2.0 g tungsten granules. The crucible was sealed and put into the induction furnace for subsequent combustion at temperatures above 1800 °C in a pure oxygen stream. The carbon and sulfur contents are calculated from the peak height and area of the absorption signals of the infrared cells.

The free calcium oxide content was determined on ground samples with a grain size below 63 μm according to EN 450–1; the chloride content was measured by potentiometric titration with silver nitrate solution according to EN 196–2. Further chemical analysis was performed by X-ray fluorescence using a Panalytical Axios X-ray fluorescence spectrometer: 0.8 g of annealed samples of the fly ashes mixed with 8.0 g lithium tetraborate LT100 to produce fused tablets using a Vulcan fusion machine 4MA by PD Instruments.

2.2.2. Mineralogical analysis

The mineralogical composition was determined using an X-ray diffractometer Panalytical X'Pert Pro with an X'Celerator detector. Data were acquired in a range of 5–70 °2θ with a step size of 0.0167 °2θ and a total measurement time of 2 h. To determine the amorphous content of the fly ashes, rutile was used as internal standard at a level of 20 wt.-%. For this purpose, the rutile powder was ground together with the fly ash sample by hand in an agate mortar until the powder was homogeneous. Rietveld refinement was performed to determine the quantitative composition of the samples using the software Panalytical Highscore Plus 4.8.

Based on the bulk chemical composition from the XRF analysis, the chemical composition of the crystalline phases according to the Rietveld refinement of the XRD pattern, and the determined amorphous content of the fly ashes the overall chemical composition of the amorphous phase was calculated.

2.2.3. Determination of the grain size distribution

The grain size distribution of 59 out of the 75 fly ashes was determined using a CILAS 1064 and a Bettersizer 3000 Plus by 3 P Instruments laser diffractometer. The samples were dried at 105 ± 5 °C until constant weight; measurements were done using ultrasonic dispersion of the powders in isopropanol.

2.3. Reactivity testing by relative compressive strength

The compressive strength of mortar samples was determined according to EN 196–1 after 28 and 90 days for specimen without and with fly ash. The reference mortar contains water, cement and aggregates in the weight ratio of 0.5:1:3. The relative strength, also called activity index (AI), of mortar containing fly ash at a level of 25 wt.-% of the binder was determined according to EN 450–1. As reference cement a CEM I 42.5 R provided by one plant was used which meets the requirements according to EN 450, but it has to be addressed, that due to the large timespan of the sampling, different batches of the reference cement were used. For each batch reference mortars were tested several times. The average of reference mortar compressive strength at 28 and 90 days is 50.0 and 56.3 N/mm^2 respectively with a standard deviation of 2.5 N/mm^2 each. The averaged standard deviation of the reference mortar compressive strength at 28 and 90 days within one batch is 1,5 and 2,0 N/mm^2 respectively showing that there is no significant change in compressive strength between the different batches.

2.4. Reactivity testing using the R^3 test method

Since some of the tests were already started before publication of the final test procedure [7,10], the composition of the R^3 system used in these investigations was adapted from Snellings et al. [3] (see Table 2).

Isothermal calorimetry was used to measure the cumulative heat of reaction of 30 selected fly ashes in the R^3 system. An isothermal calorimeter TAM Air by TA Instruments set at 40 °C and equipped with admix ampoules for internal mixing was used to perform the measurements. According to Table 2, a batch of fly ash, portlandite and gypsum was premixed for 24 hours in an overhead mixer to achieve a homogeneous sample. 3 g of this powdered sample were put in the glass ampoules and 2.7 g of 0.5 mol/l KOH solution were weighed into the syringes before loading the samples in the calorimeter. In later investigations, the corresponding proportion of the solids was weighed directly into the glass ampoules and premixed with a spatula. After the equilibration of the system the measurement was started by injecting the liquid into the powder and mixing internally for two minutes. At least two replicates were measured for a total measurement time of 9 days for each fly ash. Corresponding to the ASTM C1897 the heat release during the first 75 min was neglected. The difference from the actual ASTM protocol, which uses external mixing, is a slower mixing speed and smaller sample size used here. A possible heat loss from channels equipped with the internal mixing device was considered using the TAM

Table 2
Compositions of the R^3 test mixtures.

component	R^3 test adapted from [3]
fly ash	5 g
portlandite	15 g
gypsum	adjusted to Al_2O_3 content of the fly ash (mass ratio of SO_3: $Al_2O_{3,\text{ fly ash}} = 1$)
solution	0.5 mol/l KOH
mass ratio of solution: solids	0.9

Table 1
Overview of the 75 fly ash samples.

Plant No.	1	2	3	4	5	6	7	8	9	10	11	12	13	14	15
samples taken	20	4	1	4	11	7	19	2	1	1	1	1	1	1	1

Airs “gain factor” calibration.

2.5. Statistical evaluation

Pearson correlation of the resulting data matrix and statistics on columns has been performed using OriginLab Origin 2019b [17]. The correlation coefficient R given in scatterplots and graphics refer to Pearson if not stated otherwise. As the interpretation of correlation coefficients is not uniform and depends on the assessed data [18], in this work, the following wording is used to describe the strength of the correlation (significance level α of 0.05 ($p \leq 0.05$)): R is referred to as weak for $0.2 < |R| \leq 0.4$, moderate for $0.4 < |R| \leq 0.6$, strong for $0.6 < |R| \leq 0.8$, and very strong for $0.8 < |R| \leq 1.0$. To account for the multitude of possible influencing factors and therefore to analyze the relationship between several independent variables (chemical and physical characteristics) on one dependent variable (reactivity), multiple regressions were conducted using the Minitab® 18 Statistical Software. Factors were added to the regression term using forward selection with an α value of 0.01 for term acceptance. The model quality was rated by correlation coefficients, normal distribution of residues and its predictive quality by 5-fold cross validation method. To display the model performance the adjusted R^2 (adj. R^2) is used, which considers the model complexity and corrects R^2 for the number of independent variables.

3. Results and discussion

A multitude of tests was performed on the 75 fly ashes. The most important results regarding the scope of this paper – properties and reactivity – are presented in this chapter. However, a number of data will not be presented, but are provided in the electronic supplement to allow for further evaluation of the data. For the fly ash composition, it has to be noted that sampling numbers differ between the plants (see Table 1). However, it must be emphasized here that this does not affect the overall correlations between properties and reactivity that are the focus of this work.

3.1. Chemical and mineralogical properties and their intercorrelations

3.1.1. Chemical composition

Although the fly ashes originate from different plants most of the chemical parameters show a normal distribution according to the Kolmogorov-Smirnov test with a significance level of 0.5, however, in the Shapiro-Wilk test the results are varying. Performing the “two-sample t-test” with the chemical composition of the fly ashes of the plants with the highest number of samples (plant 1 & 7), it was found that most of the parameters do not belong to the same statistical population. As stated above this does not bias the overall correlations between the properties and reactivity. The distribution of the LOI and the $SiO_2+Al_2O_3+Fe_2O_3$ content of the fly ashes assigned to the different plants are illustrated in Fig. 1 and Fig. 2 exemplarily.

According to EN 450–1 fly ashes are categorized in three LOI (loss on ignition) classes. All but one fly ash tested in this study do fulfill the requirements: 63 fly ashes can be attributed to category A (LOI < 5.0 wt.-%), 8 fly ashes fit into category B (LOI < 7.0 wt.-%) and three fly ashes fall into category C (LOI < 9.0 wt.-%). One fly ash showed a loss on ignition of 9.61 wt.-%.

Fig. 3 depicts the correlation of the carbon content of the fly ash with the LOI. It is evident, that the unburnt carbon from the fly ash is the main reason for the LOI and therefore the assignment of the ashes to the according categories.

The average chemical composition of the 75 fly ashes determined by X-ray fluorescence is shown in Table 3. Additionally, the minimum and maximum contents are displayed. The underlying data of the individual samples can be found in the electronic supplement. Using X-ray fluorescence and diffraction data, the chemical composition of the amorphous phase of the fly ashes was calculated and is also shown in Table 3.

Apart from the requirements concerning the LOI, all other chemical parameters are in accordance with EN 450–1. The sum of the oxides, which is supposed to be relevant for the pozzolanic reaction (SiO_2, Al_2O_3 and Fe_2O_3) is 77.9–89.8 wt.-%, 84.3 wt.-% on average. The distribution of the main oxide contents and the content of the amorphous phase can be found in the electronic supplement 2.

3.1.2. Mineralogical composition

The amorphous content of the samples is in the range of 56–92 wt.-%

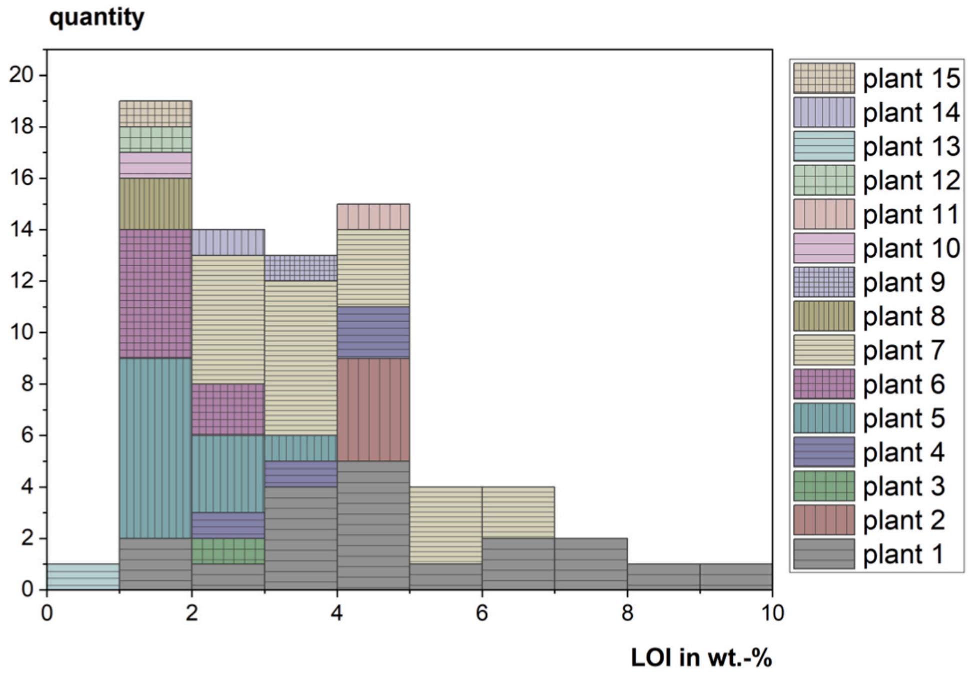

Fig. 1. Distribution of the LOI content of the fly ashes assigned to the different plants.

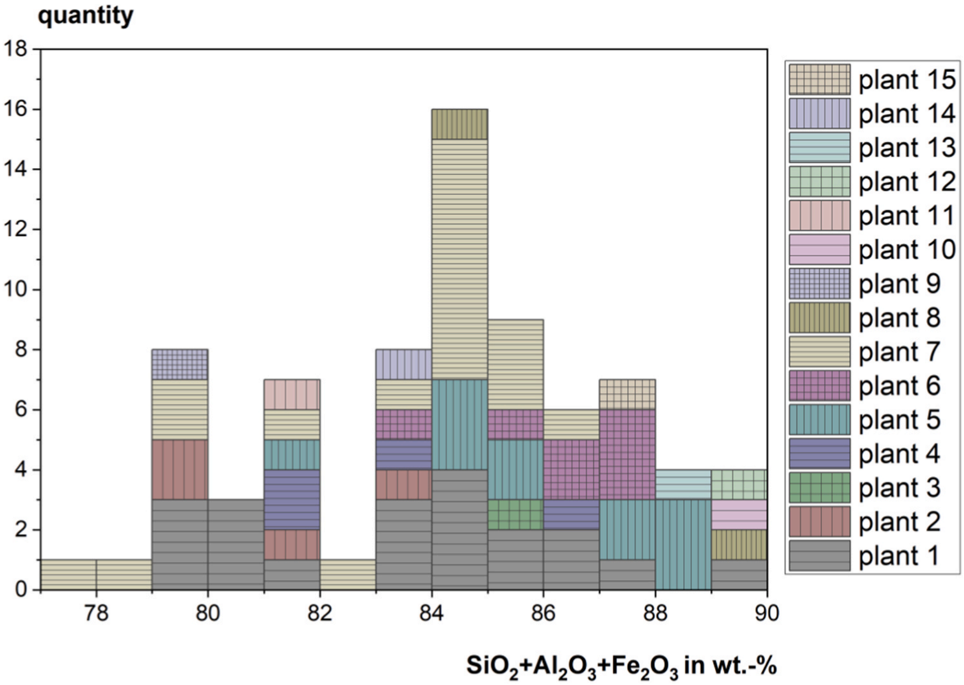

Fig. 2. Distribution of the $SiO_2+Al_2O_3+Fe_2O_3$ content of the fly ashes assigned to the different plants.

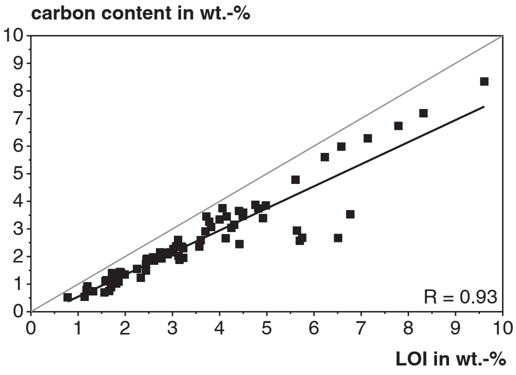

Fig. 3. Carbon content in correlation with loss on ignition.

Table 3
Overview over the chemical composition of the fly ashes and their amorphous proportion.

Oxide	fly ash minimum and maximum contents in wt.-%	amorphous proportion minimum and maximum contents in wt.-%^{1})
SiO_2	46.9–61.0	45.2–62.3
Al_2O_3	20.0–31.7	9.80–26.4
Fe_2O_3	3.59–10.4	3.70–11.7
CaO	2.14–6.50	2.57–8.92
MgO	1.16–3.28	1.43–4.08
TiO_2	0.83–1.95	0.98–3.31
SO_3	0.24–2.12	0.00–1.24
P_2O_5	0.24–2.41	0.33–4.09
Na_2O	0.21–1.84	0.68–4.70
K_2O	0.82–4.16	1.39–5.66

1) related to fly ash glass.

(average 72.9 wt.-%). As main crystalline phases mullite (average 12.8 wt.-%), quartz (average 10.6 wt.-%), magnetite (average 1.58 wt.-%), hematite (average 0.86 w.-%), bassanite (average 0.25 wt.-%) and bloedite (average 0.17 wt.-%) could be identified. Minor phases with a content of less than 1.0 wt.-% in all fly ashes were periclase (≤ 0.8 wt.-%), free lime (≤ 0.7 wt.-%), gypsum (≤ 0.4 wt.-%), anhydrite (≤ 0.8 wt.-%) and sylvine (≤ 0.2 wt.-%).

Quantifiable amounts of bloedite ($Na_2Mg(SO_4)_2 \cdot 4\ H_2O$) were found in five samples of plant 7 (bloedite content: 1.3–1.7 wt.-%) that show the highest contents of SO_3 throughout all the ashes (SO_3 content: 1.5–2.1 wt.-%). The presence of bloedite in these samples seems to be accompanied by a higher content of bassanite (1.0–1.6 wt.-%). The elevated LOI of these ashes suggests that they were produced by burning sulfur rich coal at relatively low temperatures [19,20]. Further research into the source of these ashes revealed that they were produced by mixing a regular ash with a second-grade ash from a dump.

3.1.3. *Correlations*

The CaO in the glass component of the fly ashes was found to correlate with the content of CaO in the overall fly ash. Around 90% of the CaO of the fly ashes was found in the amorphous phase. The correlation is depicted in Fig. 4.

Interestingly, the amount of TiO_2 in the fly ash affects the precipitation of mullite in the formation process of the fly ash. Fig. 5 depicts the correlation between the mullite content and the amount of TiO_2 present

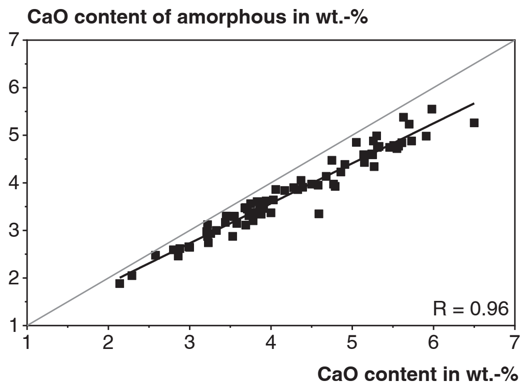

Fig. 4. Content of CaO in the amorphous phase of the fly ashes in correlation to the total CaO content (both related to the weight of fly ash).

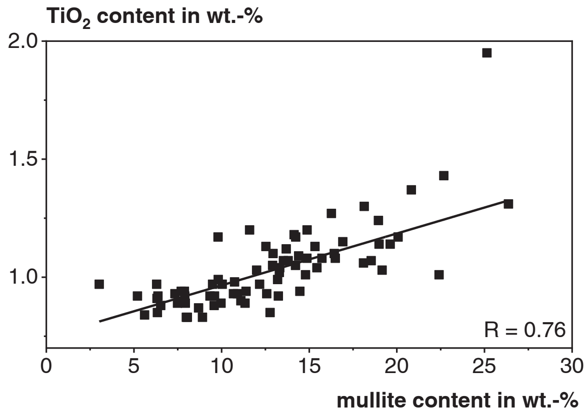

Fig. 5. Correlation between TiO_2 content and mullite content of the fly ashes.

in the ashes examined in this study. This agrees with the study by Montoya et al. where a higher content of TiO_2 leads to an enhanced formation of mullite. Most likely this happens during the cooling of the ash at the electrostatic precipitator. Montoya et al. reported, that Ti^{4+} enters the mullite microstructure and forms a Ti^{4+}-mullite solid solution [21]. Baudin et al. showed, that the addition of TiO_2 enhances the grain size of mullite during sintering [22], possibly leading to an increased amount of mullite formed during the process. Lu found that mullite content is enriched in the coarser fly ash fractions [23].

3.2. Physical properties

It is well established, that the replacement of Portland cement with fly ash leads to an increase in the total porosity of the hydrated product but to a decrease of the average pore size [24,25]. Thereby, the physical properties in terms of grain size distribution and specific surface have a decisive influence on the reaction kinetic and microstructure development. Chindaprasirt et al. showed, that blended cement pastes containing a classified fly ash with a smaller average grain size have a higher compressive strength than cement pastes containing the original fly ash [26].

In this study, the grain size of the fly ashes was determined using laser diffraction. 59 of the 75 fly ashes of this study were examined. The results are depicted in Fig. 6.

The at least trimodal distribution of the incremental grain size distribution can be associated with the process of the electrostatic precipitation in the power plant. In the direction of flue gas exhaustion several hoppers collect the fly ash particles into containers [27]. These containers are subsequently emptied into a silo when they are full. This results in different layers of fineness within a silo and causes the multimodal grain size distribution. The multimodal grain size distribution has also been discussed elsewhere [14,28,29].

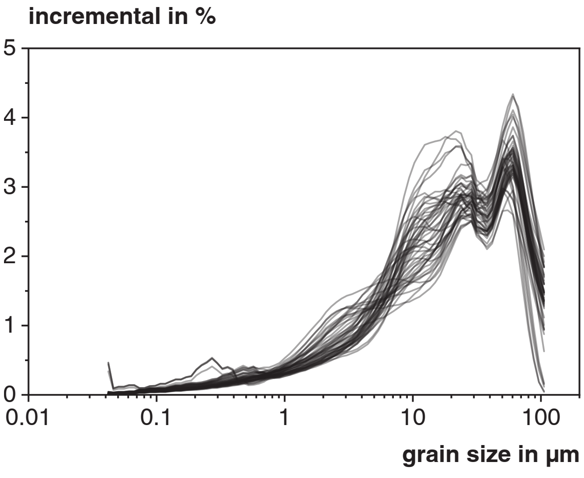

Fig. 6. Particle size distribution – overview on 59 fly ashes.

The average grain size of the fly ashes examined in this study was $d_{50} = 21.74$ µm with 3.20 µm standard deviation, 10% of the particles were smaller than $d_{10} = 2.53$ µm with a standard deviation of 0.66 µm, 10% were bigger than $d_{90} = 78.56$ µm with 10.80 µm standard deviation.

3.3. Reactivity testing by relative compressive strength

3.3.1. Overview

The relative strength of a mortar containing SCM and OPC in relation to a mortar prepared using pure Portland cement is often used as a benchmark to determine the reactivity of SCMs. When looking at a certain type of SCMs, e.g. fly ashes, the influence of the cement on the reaction of the SCM becomes more pronounced, resulting in relative strengths that are very similar. Fig. 7 shows the relative strength of the fly ashes evaluated in this study after 28 and 90 days of hydration. Most of the relative compressive strength data are in the range of 0.8–1.0 for 28 days and 0.9–1.2 for 90 d. The average 28-day relative compressive strength is 0.915 with 4.9% standard deviation from mean. After 90 days the average is 1.047 with a standard deviation of 5.4%. All results are in the range of the plants with numerous samples (plant 19 & 20). It becomes obvious, that high reactivity cannot be assigned to particular plants. Fly ashes from the same source vary significantly as is visible for plant 1, 5, and 7.

3.3.2. Correlations

No robust correlation between the chemical or the mineralogical composition or the amount of amorphous phase in the fly ash with the relative strength could be found. Minor influencing tendencies on the 90 days AI ($0.25 < |R| < 0.35$, $p < 0.05$) were calculated for MnO, Fe_2O_3, $Al_2O_{3\text{glass}}$, $Fe_2O_{3\text{glass}}$, $SO_{3\text{glass}}$, periclase, free lime, gypsum, bloedite and calcite; while the 28 days AI seems slightly more dependent on bulk composition parameters with $0.25 < |R| < 0.55$ for CaO, Fe_2O_3, $SiO_2+Al_2O_3+Fe_2O_3$, CaO_{glass}, $Fe_2O_{3\text{glass}}$, $SiO_{2\text{glass}}$, $SiO_{2\text{glass}}+ Al_2O_{3\text{glas}}+ Fe_2O_{3\text{glass}}$, periclase, and bassanite. Based on the large data base it cannot be confirmed that the glass content itself has a major influence on the strength activity index, as can be seen in Fig. 8. It is well known that fly ash is composed of different glasses [38]. Not only the total amorphous share but rather the composition of the glass phase, which contains network building oxides and glass network modifiers that are determining solubility and therefore fly ash reactivity are affecting strength development. Thus, also glass composition parameters, e. g., expressed by the NBO/T relation (non-bridging oxygen atoms / tetrahedral network forming ions [38], further discussed in chapter 3.4) or the N_r (ratio of network modifiers to network formers [34], further discussed in chapter 3.5.1), were considered in the search for correlations. They showed a similar pattern and correlation factors of only $R = 0.14$ and $R = 0.23$, respectively.

Also, for the physical properties only a slight tendency with $R = -0.33$ for the parameter "Fineness according to EN 450" could be found between grain size parameters and the relative strength of the mortars after 90 days. Exemplarily this is depicted for the median particle size and the fineness according to EN 450 in Fig. 9. Due to the general fineness of the fly ash particles they dissolve over time so the impact of particle size might be visible for short time but attenuates for long time strength. A higher correlation might be found for a shorter period, e.g., 7 days strength. However, at an early age, the effect as a nucleation substrate for reaction products which accelerates hydration can overshadow the reactivity of the fly ash itself.

It was already stated by Snellings et al. [3], that the specific surface area of SCMs of different origins is not the main determining factor for reactivity in terms of strength development and the effect of bulk composition and (glass-)solubility is relevant as discussed above. Since

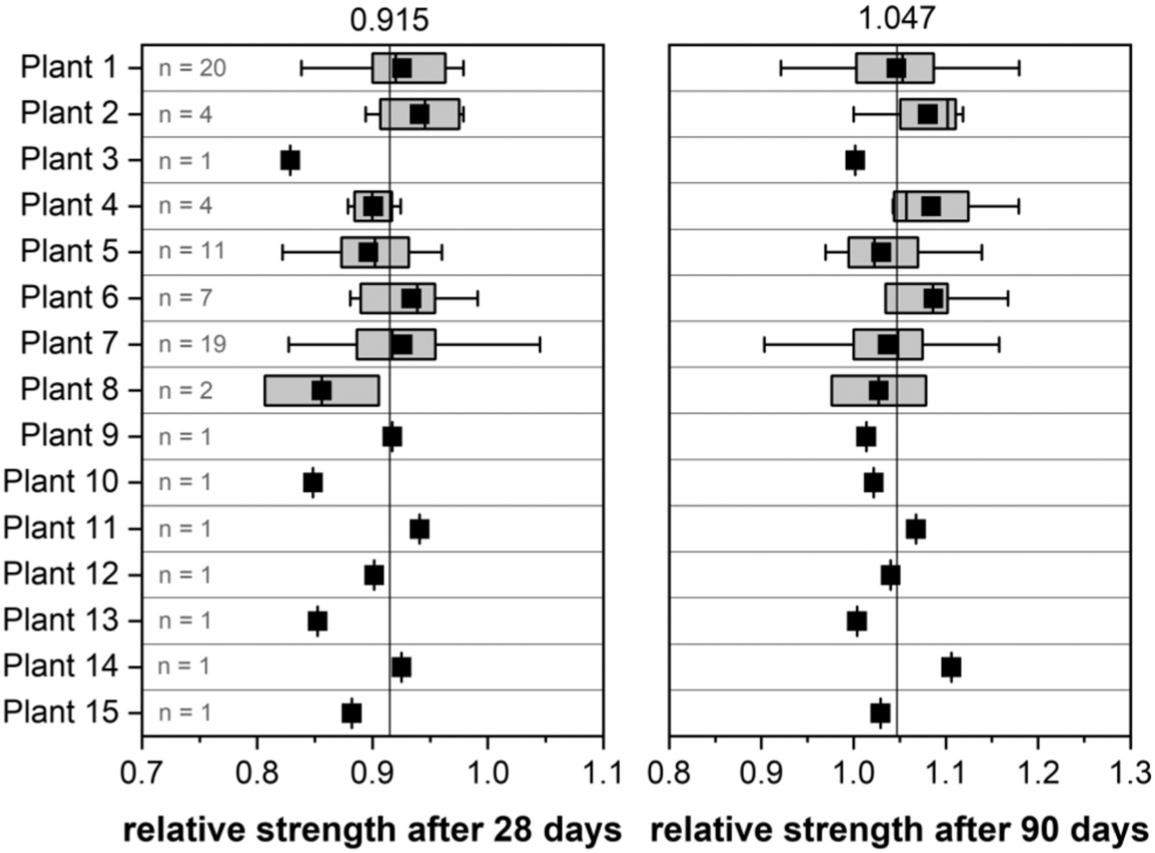

Fig. 7. Box plot of the relative compressive strength after 28 and 90 days (square: average, line: median, box: standard deviation, whiskers: min/max).

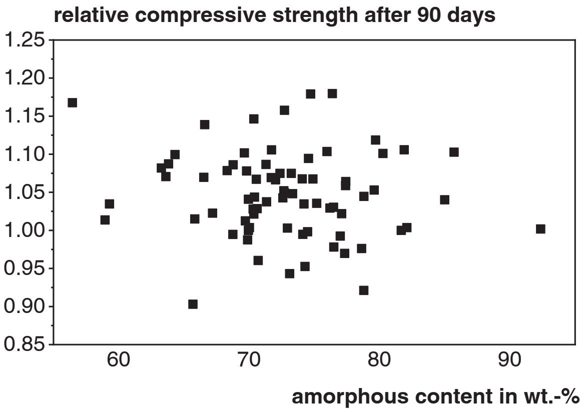

Fig. 8. Plot of relative strength after 90 days versus the amorphous content of the fly ash.

the reactivity obviously depend on several factors a multiple regression analysis was carried which is described in detail in the electronic supplement 2. However, no sufficient fit could be generated by using bulk- and glass composition parameters as independent variables. With the best fit, only 27% of the data were explained by using Al_2O_3 and Fe_2O_3.

The manifestation of the factors in the relative compressive strength in this study might be superimposed by the influence of the cements used and different production times and conductors. The relatively bad reproducibility of the AI in comparison to the range of variation of the relative compressive strength data (e.g. all data for 28 days here are in the range from 0.8 to 1.0) makes this method not suitable to precisely assess materials with relatively similar reactivity.

3.4. *Reactivity testing using the R^3 test method*

The R^3 heat calorimetry test has been designed to directly measure pozzolanic reactivity without the influence of cement within a relatively short time. It has been shown for a large group of SCMs that the heat of reaction in the R^3 system is a good indicator for the reactivity [3,5]. Therefore, it was assumed that the same applies for the reactivity of fly ashes.

Snellings et al. proposed two distinctive time intervals, 2.8 days and 9 days, as indicator for the relative strength of mortar with SCM at 28 and 90 days [3]. In this study the total heats of reaction at those times were chosen as parameters. As expected, the data of those intervals correlate quite well with each other (cf. Fig. 10). It therefore can be stated, that a test duration of around three days is enough to predict the heat of reaction at later times reasonably well at least for fly ashes ($R = 0.97$). However, it has to be considered that other SCMs may show a different correlation between these two testing times.

Fig. 10 also shows that the heat of reaction is quite different for the investigated fly ashes. Minimum and maximum differ by a factor of 3.8 after 2.8 days and 4.3 after 9 days. Consequently, the test has a much higher resolution in reactivity assessment compared to the strength activity index. Londono-Zuluaga et al. found a similar trend for the recent R^3 test [10] where the heat release for fly ashes after 7 days ranged from about 160–360 J/g SCM for fly ashes and for calcined clays up to more than 1000 J/g SCM [8].

Fig. 11 shows the relative compressive strength vs. the heat of reaction in the R^3 test. The 2.8-day heat release is supposed to correlate with the 28 days strength and the 9 days heat release with the 90 days strength. The figure shows a weak trend towards higher relative strength at higher heat release, but the scatter is very large. Within each individual time step, no correlation can be found (AI_{28d}-$Heat_{2.8d}$: $R = 0.25$; AI_{90d}-$Heat_{9d}$: $R = 0.04$; both not significant on a level of $p = 0.05$).

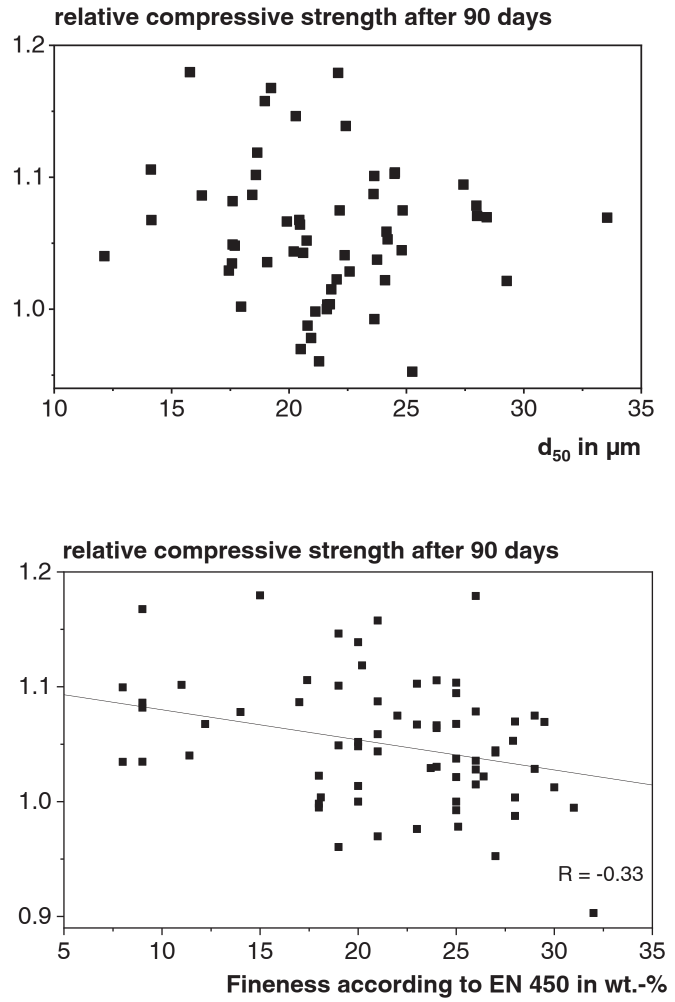

Fig. 9. Relative strength after 90 days in relation to particle size and fineness (> 0.045 mm according to EN 450) of the fly ash.

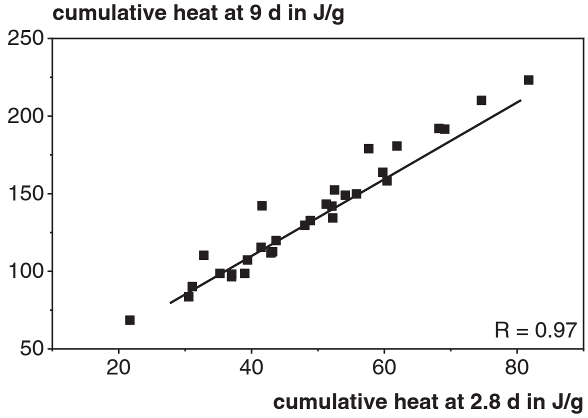

Fig. 10. Correlation between cumulative heats in the R^3 system released after 2.8 and 9 d.

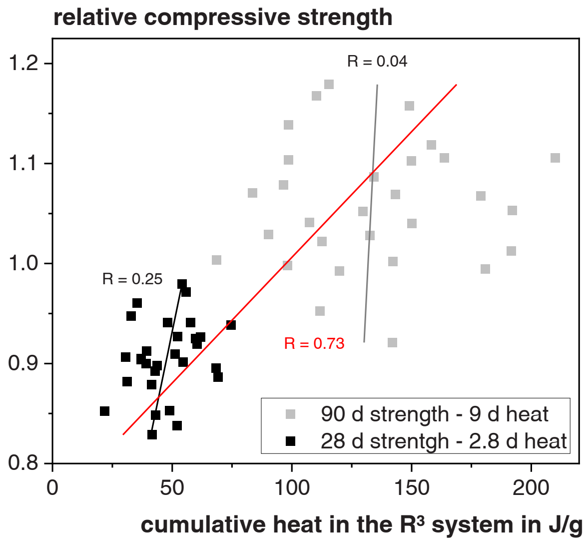

Fig. 11. Relative compressive strength plotted against cumulative heat in the R^3 system released after 2.8 and 9 days.

Inaccuracies in the method of determining the compressive strength of standard mortars as discussed in chapter 3.3 could also contribute to the poor correlations with relative compressive strength. Furthermore, it is not clear how the sulfate adjustment effects the correlation to strength as more Al_2O_3 and consequently more sulfate in the system should lead to more ettringite formation which is not comparable to reactions occurring in a blended cement system. However, Snellings et al. [3] found that the test correlates with the compressive strength of blends with fly ash and other SCMs. But the fly ashes used in their study differed much more in compressive strength.

Apart from relative strength, there are other factors, which are related to the heat released during reaction in the R^3 system. E.g., Pearson correlation revealed a correlation between the MgO content of the fly ashes and the cumulative heat after 2.8 and 9 days, as can be seen in Fig. 12 exemplarily for the heat of reaction after 9 days.

All tendencies and correlations, found for chemical, mineralogical, and physical characteristics to cumulated heat after 9 days in the R^3 test, significant on a level of $p = 0.05$, and additional selected parameters, of which correlations were initially expected, are summarized in Table 4 with the correspondent Pearson R. An additionally conducted Spearman correlation calculation showed no substantial differences.

The alkali content, expressed as Na_2O_{eq}, expectedly showed no severe influence on the reactivity as KOH is provided in high amounts in the R^3 test. Except for chloride, all found determinants are well known from literature discussions, as part of different reactivity indexes and from model proposals. E.g., ASTM C618 specifies a minimum amount of 50 wt.-% of SiO_2+Al_2O_3+Fe_2O_3 for fly ashes and of 70 wt.-% for natural pozzolans to ensure the respective pozzolanic reactivity [31]. This comparably unspecific parameter was already found to entail drawbacks in reactivity prediction because it firstly does not describe the amorphous proportion of these oxides and secondly only accounts for

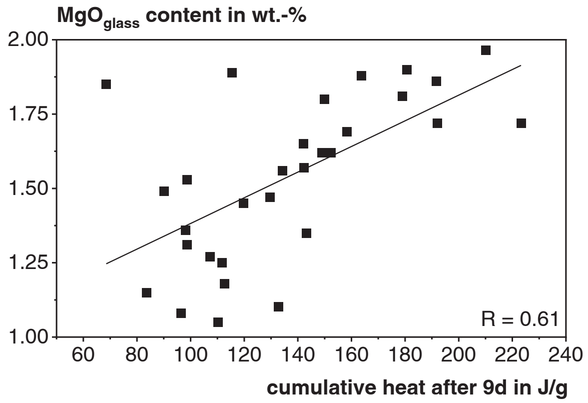

Fig. 12. Influence of the MgO content on the cumulative heat after 9 d of reaction in the R^3 system.

Table 4
Correlations to cumulated heat after 9 d in the R^3 test.

Variable		Pearson R
Constituent of the FA (contents in wt.-%)	**Cl^-**	**0.62**
	CaO_{free}	*-0.39*
	MgO_{total}	**0.53**
	Na_2O_{eq}	*0.12*
	$Al_2O_{3\ total}$	*-0.36*
	$SiO_{2\ total}$	*0.34*
	Fe_2O_3	-0.25
	$TiO_{2\ total}$	**-0.50**
	MnO_{total}	**0.68**
	mullite	**-0.50**
	glass	*0.26*
Constituent of the FA glass (contents in wt.-%)	$Al_2O_{3\ glass}$	*0.35*
	$TiO_{2\ glass}$	**-0.50**
	MgO_{glass}	**0.61**
	Fe_2O_3	-0.27
	$SiO_{2\ glass}$	*0.26*
Particle size	d_{50} in µm	-0.46
Reactivity indexes	ASTM C618 index ($SiO_2+Al_2O_3+Fe_2O_3$) in wt.-%	0.28
	N_r [-] after [31]	*0.01*
	NBO/T [-] after [36]	*-0.18*
	K-value [-] after [37]	*-0.10*
	NBO/Si [-]	*-0.13*

**italic*: not significant on a level of p=0.05

network building oxides and does not include glass network modifiers. These network modifiers are known to determine the fly ash dissolution and therefore the reactivity in cementitious and alkali activated systems [16,32–36]. They destabilize the glass network by so-called nonbridging oxygen atoms (NBOs) by disconnecting the silicate connections and therefore increasing disorder which promotes solubility [33]. In order to account for the network modifiers, different index proposals, referring to a known glass chemistry ratio ($\frac{NBO}{T}$; $\frac{NBO}{Si}$, where T represents tetrahedral network forming ions, Si is SiO_2) [37,38] can be found in the literature. E.g., Durdzinski et al. [38] are using the NBO/T ratio, Shekhovtsova et al. [39] are using a variant of Si/NBO including shape and particle size distribution, the so-called "K-value" to assess reactivity of fly ashes for alkali activated materials. For cementitious systems Oey et al. proposed an index, the so-called "network ratio (N_r)" which uses the ratio of network modifiers to network formers present in the fly ash glass. The 7-day heat release of a mix of 50% fly ash / 50% OPC of seven fly ashes investigated in the study of Oey et al. correlated well with the introduced network ratio N_r [34]. N_r is calculated following Eq. 2 and 3 or simplified by Eq.4:

$$N_r = \frac{2\cdot\left(X_{Ca} + X_{Mg}\right) + X_K + X_{Na} - X_{Al}}{X_{Si} + X_{Al}} \tag{2}$$

and

$$N_r = 0\text{for}\left[\frac{Al_2O_3}{M_2O + M'O}\right] > 1 \tag{3}$$

$$N_r = \frac{X_{Ca} + X_{Mg} + X_K + X_{Na}}{X_{Si} + X_{Al}} \tag{4}$$

where X_{Ca}, X_{Mg}, X_K, X_{Na}, X_{Al}, and X_{Si} are the mole fractions of calcium, magnesium, potassium, sodium, aluminum, and silicon in the fly ash glass; $M_2O+M'O$ is the share of alkali (M) and alkaline earth (M') cations present in the glass, expressed in wt.-% [33].

Regarding the correlations found in this study MgO is known as a network modifier and therefore enhancing dissolution of fly ash glass; MgO is considered in [33], MnO in fly ashes will react in the same way as MgO [35], while Al_2O_3, TiO_2 and SiO_2 are well known as network builders. The influence of grain size (d_{50}) and the mullite content were discussed earlier in this work.

Although the introduced indices comprise the same factors, that were identified as relevant for the measured heat release in the R^3 test, the reactivity seems not well described by these indices (see Table 4). Therefore, a multiple regression to describe the heat development by an empiric model was conducted.

When looking at correlations between mineralogical, physical and chemical characterization data to reactivity and strength development, it has to be considered that these measures only refer to bilateral, monotonic correlations and also that these "input" parameters are partially interrelated between each other. Fig. 13 gives an overview over the correlations (Pearson) found for the chemical and physical parameters of the 75 fly ashes characterized in this work. It is revealed, that the manifestation of most parameters seems to be codetermined by the plant they are produced at, which might be due to differing fuel compositions or process parameters. The correlations of Table 4 are not to be considered as the only, respectively compulsory, determining factors for the heat release in the R^3 system as, e.g., bulk aluminum content is related to titanium content, chloride is slightly but significantly correlating to magnesium, which in turn shows connections to manganese.

Multiple linear regression analysis coefficients, conducted for different units (wt.-$\%_{total}$, wt.-$\%_{glass}$, mol/kg_{total}, mol/kg_{glass}, mol-$\%_{glass}$), revealed that the TiO_2 content and the content of Cl^- has the most relevant influence on the released heat after 9 days of reaction.

As can already be seen from the bilateral correlations, an increasing Cl^- content of the fly ash increases slightly the heat release, whereas an increasing TiO_2 content lowers the heat release. The regression results are depicted in Fig. 14; the calculated correlation function, Eq. (5), explains 78% of the data as can be taken from Table 5. It has to be noted, that the exclusion of two datasets (samples with unexpectedly low cumulative heat measured) from the regression improved the fit by 42%.

$$Q_{9d} = -5.3 + 912\ Cl^- + \frac{139.5}{TiO_2} \tag{5}$$

Where Q_{9d} is the cumulated heat after 9 days in the R^3 test in J/g, Cl^- is the chloride content referred to the glass in mol-%, and TiO_2 is the fly ash titanium oxide content referred to the glass content in mol-%.

The apparent determining role of titanium with a negative correlation to the heat of reaction might be explained rather by its relation to mullite and the concomitant effect on amorphous aluminum content than by its function as a network forming element. A similar effect can be observed during the reaction of blast furnace slag [30]. As described earlier in Fig. 5, the presence of titanium promotes mullite formation in the combustion process. This theory is underlined by the moderate correlation of total aluminum to mullite ($R = 0.66$, $p < 0.0001$), respectively titanium ($R = 0.75$, $p < 0.0001$) in contrast to the negative correlation of amorphous aluminum to mullite ($R = -0.78$, $p < 0.0001$) and titanium ($R = 0.72$, $p < 0.0001$). Similar findings were already drawn by Lu in 1986; a decreasing amorphous Al_2O_3 content was associated with increasing mullite content [23]. Silicon as the second element of mullite only correlates weakly, as other sources, e.g., quartz, cristobalite, or amorphous components are present in the fly ashes, too.

(Calcium-) chloride is known as a good hydration accelerator [40] and discussed in numerous publications. This accelerating effect could cause the correlation to higher heat release in the R^3 test. E.g., amounts of 1 wt.-% of cement (effective chloride content 0.64 wt.-%), were found to increase 28- and 90-days compressive mortar strength by 30% respectively 36% [41]. Giergiczny proved, that also for fly ash – $Ca(OH)_2$ pastes, $CaCl_2$ works accelerating and therefore promotes heat release [42]. Already 0.0006 wt.-% (related to cement content) of $CaCl_2$ affect the early age 1–3 d hydration process. In the study of Venkateswara et al. [43], potassium chloride addition improved 28 days compressive mortar strength by 16%. Transferred to the chloride content determined for the fly ashes in this work an increase of 2–6% could be expected.

However, chloride contents of the investigated fly ashes are pretty low compared to most accelerator studies. An explanation for an impact

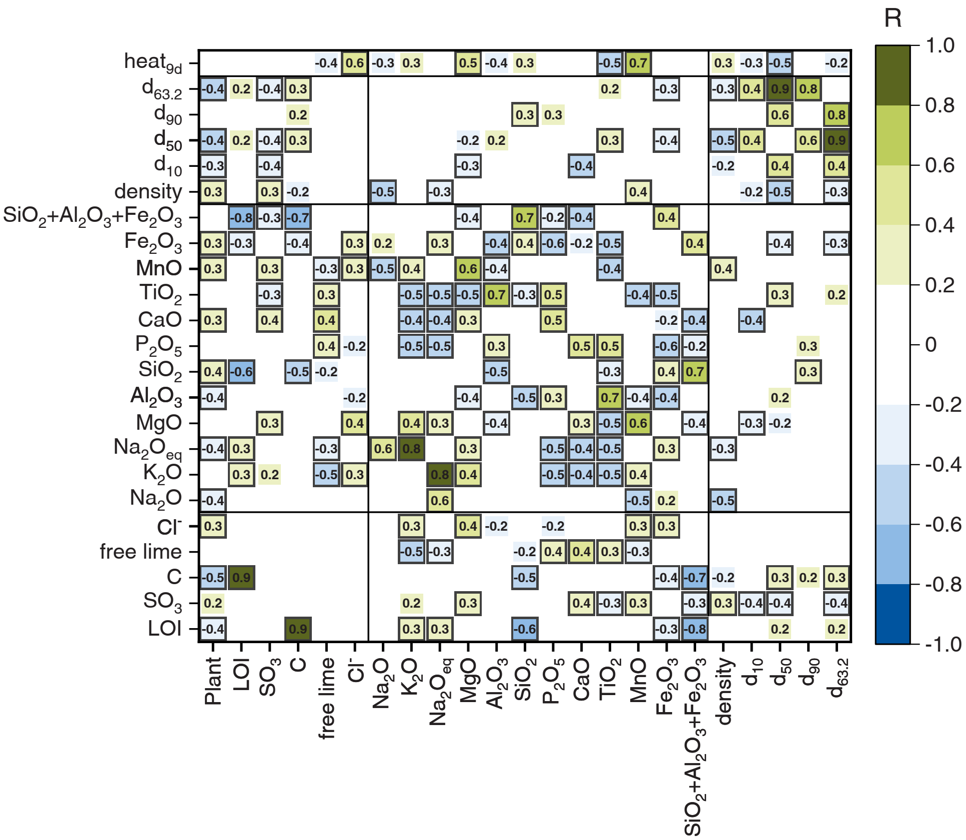

Fig. 13. Heatmap of the Pearson correlations between fly ash characterizing parameters (n = 75) and cumulative heat after 9 days in the R^3 test (n = 30); significant correlation coefficients on a level of p = 0.05 are framed black.

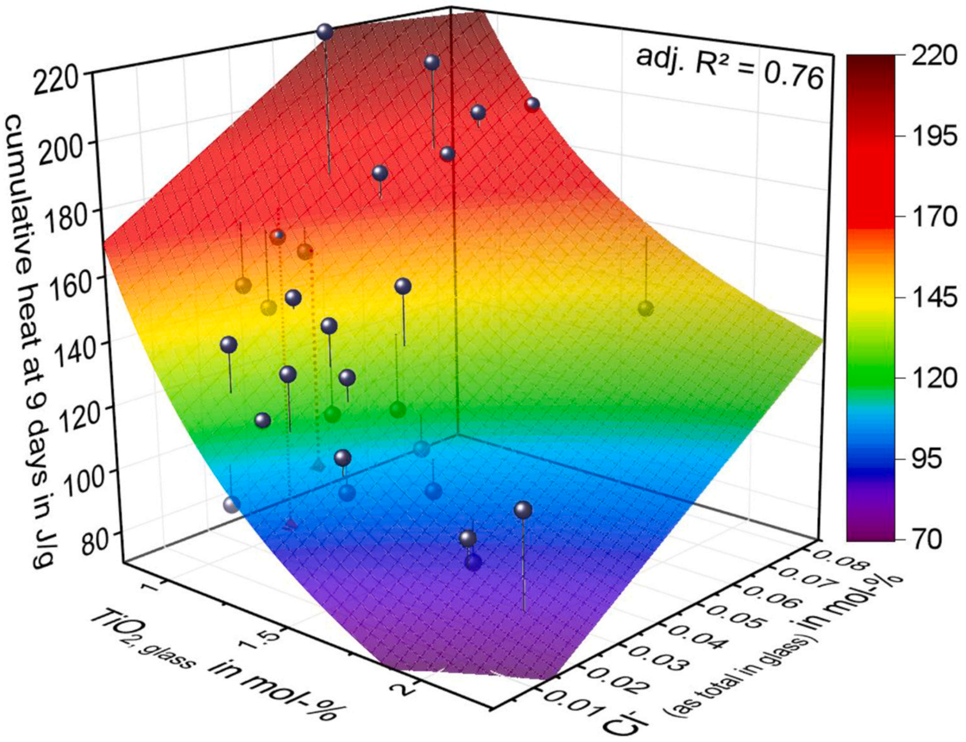

Fig. 14. Graphical representation of the multiple regression (mesh surface) of the heat released after 9 d reaction in the R^3 system in dependence of the TiO_2 and Cl^-.

Table 5

Model quality parameters for regression of chloride and titanium content in mol-% on the heat release after 9 days reaction in the R^3 test.

term	p-value	contribution	adj. R^2
Cl^- in mol-%	0,000010	27.22%	76%
$1/TiO_2$ in mol-%	0,000001	50.53%	

despite this low content could be the concentration of chlorides in the outer sphere of fly ash particles respectively as water soluble salts on the surface, which is a known phenomenon [11,44,45]. E.g., Deng et al. found 23–76 wt.-% of the total chlorine at the surface of the FA particles [44].

Besides the direct influence, the chloride content might be an indicator for the network modifiers Na, K, Ca, Mg, respectively the alkali content and distribution. Alkali salts are well known to be part of the combustion gas flow of power plants, whereby chlorides are preferably formed. When precipitating at lowering temperatures they are enriched at the surfaces of fly ash particles (and other surfaces of the plant) [11, 44,45]. A higher surface enrichment may hint towards a higher bulk alkali content which is indicated by the factor “chloride”.

Fig. 13 underlines this assumption by the statistical data of this study where chloride shows a moderate but significant linear correlation to K, Mg, and Mn where the latter in turn correlate with similar correlation coefficients to the heat released in the R^3 system (Table 4).

Also, Deng et al. found correlations of alkalis to chlorine content in six fly ashes with $R = 0.85$ for K, followed by Na ($R = 0.67$), and Mg ($R = 0.45$), suggesting a combined surface enrichment [44]. Zhu et al. found Na, K and Ca to be the main alkali chlorides in fly ashes. The speciation of chlorine in the fly ashes of that study averagely consisted of 15 mol-% NaCl, 10 mol-% KCl, and 50 mol-% $CaCl_2$. The characteristics are depending on the kind of acid gas removal and vary from 13 to 83 mol-% for NaCl, 10–32 mol-% for KCl, and 37–73 mol-% $CaCl_2$ [46].

However, inserting the alkalis as factors instead of the chloride content did not result in a comparably good fit. Therefore, it is likely that the factor “chloride content” as an indicator term is relevant in combination with the accelerating effect of chloride as reactant itself and possibly other unknown effects.

When adding oxides relevant for the pozzolanic reaction (SiO_2 and Fe_2O_3) to the model, 93% of the data can be explained as can be taken from Fig. 15 and Table 6; considering Al_2O_3 or a sum of these oxides did not improve the model. Using the unit mol.-% referred to the glass content as done for the 2-factor-model decreases the fit by 9% points. The values are therefore expressed in mol/kg of the total fly ash. Reason for this deviation might be increased error ranges due to the calculated amorphous phase contents.

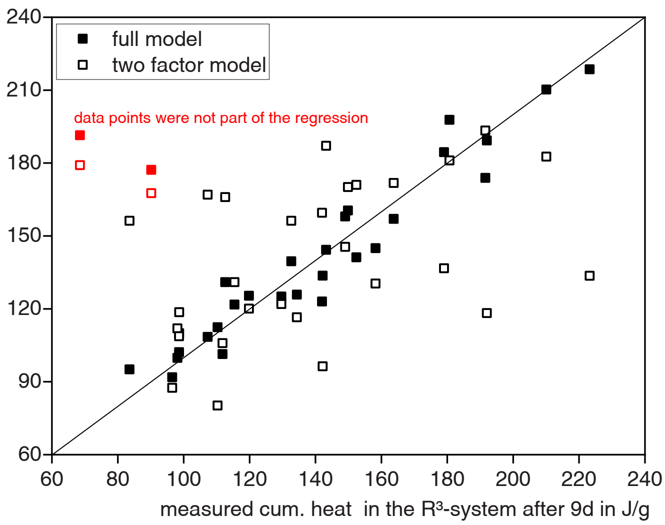

Fig. 15. Regression function and graphical representation of the multiple regression results of the heat released after 9 d reaction in the R^3 system in dependence of the content in mol per kg of TiO_2, Cl^-, Fe_2O_3, and SiO_2. Probable outlier values were not used for regression.

Table 6

Model quality parameters for regression of chloride-, titanium-, iron-, and silicon content in mol/kg on the heat release after 9 days reaction in the R^3 test.

term	p-value	contribution	adj. R^2
Cl^- in mol/kg	0.00004	24%	91%
$1/TiO_2$ in kg/mol	0.00000	46%	
Fe_2O_3 in mol/kg	0.00068	5%	
SiO_2 in mol/kg	0.00001	5%	
$Cl^- \cdot Fe_2O_3$ in mol/kg	0.00002	10%	
$1/(SiO_2 + Fe_2O_3)$ in kg/mol	0.00008	2%	

$$Q_{9d} = -664 - 81857Cl^- + \frac{22.24}{TiO_2} + \frac{3675}{SiO_2 + Fe_2O_3} + 58.7SiO_2 - 631Fe_2O_3 + 173193Cl^- \cdot Fe_2O_3 \qquad (6)$$

Where Q_{9d} is the cumulated heat after 9 days in the R^3 test in J/g, Cl^- is the chloride content in mol/kg, and TiO_2 is the titanium oxide content in mol/kg, SiO_2 is the silicon oxide content in mol/kg, and FeO_2 is the iron oxide content in mol/kg.

Considering an unneglectable source of error due to the heterogeneous material, different testing times, different operators, several laboratory samples of one fly ash, method combinations, and the indirectly determined values, the models seem satisfying.

4. Summary

In this study 75 siliceous fly ashes were analyzed concerning their chemical, mineralogical and physical properties. To identify relevant parameters influencing the reactivity of fly ashes and their contribution to strength development in cement - fly ash mixtures, the relative compressive strength (activity index) determined on cement - fly ash mortars and heat calorimetry measurements of fly ash reaction in an alkaline environment (old version of the R^3 test) were conducted. The results were then statistically evaluated by the means of a Pearson correlation and multiple regression calculations. The main findings of the study can be summarized as follows:

- Chemical, mineralogical and physical properties of siliceous fly ashes partly depend on the plant they are produced at. However, they can vary vastly within one plant. As the power plant and fly ash separation technologies used in Germany are very similar, the different properties of fly ash are caused by the coal used, the grinding fineness of the coal before combustion, and the co-combustion of secondary fuels. Hard coals fired in Germany are mixes from the worldwide market and therefore can vary in properties from batch to batch.
- Contrary to literature, the heat release in the used version of the R^3 test show weak (2.8 d, $R = 0.22$) to no (9 d, $R = -0.0038$) correlations to the relative compressive strength. This might be explained by the relatively low variation of composition when looking at just one type of SCM and the superimposing effects of the test cement in relative compressive strength testing. When having SCMs with relatively similar reactivity, the reproducibility of relative compressive strength testing does not allow a clear distinction of different reactivities; in contrast, the R^3 test has a better resolution. Furthermore, the sulfate adjustment in the used version of the R^3 test may impact the correlation to strength negatively.
- Against initial expectations, no strong bilateral correlations could be found between the relative mortar strength or the heat released in the used version of the R^3 test and the glass content or the fineness of the examined fly ashes.

- However, the heat release after 9 days in the used version of the R^3 test can be sufficiently well described by multiple regression functions based on bulk composition factors. Using chloride and titanium oxide contents, 78% of the data can be explained. Similar to blast furnace slag, higher TiO_2 content results in a lower heat released in the R^3 test, which indicates a reduced reactivity of those ashes, whereas a high chloride content maps a higher fly ash reactivity. Adding silicon- and iron oxide contents to the two-factor model function improves the fit to 93%.

5. Conclusion and outlook

In conclusion, the statistical analysis showed that no strong bilateral correlations could be found between the reactivity of the fly ashes and their chemical, mineralogical and physical properties, which demonstrates the complexity of their relationships. The effects of several parameters are overlaid. The multiple regression analysis showed that less expected parameters such as chloride and titanium appear to be the most relevant. However, their exact influence on the reaction and the role of the other parameters usually considered relevant is still not clear. On the one hand, deeper research into the reaction mechanisms and the influence of the relevant parameters on the microstructure development will enhance the understanding. On the other hand, it would be interesting to validate and, if required, improve the derived function by applying it to more fly ashes with different composition. Moreover, it should be investigated if the function is transferable to the current R^3 test according to ASTM C1897–20. Although the R^3 test is a comparably rapid method to determine reactivity, the assessment based on bulk composition would be a time-saving option. However, since the cement used has a huge superimposing effect on the strength development, the prediction of the latter is still a difficult topic and the reactivity assessment could be more relevant for applications with high fly ash usage.

CRediT authorship contribution statement

Thomas Matschei: Writing – review & editing. **Steffen Overmann:** Writing – original draft, Visualization, Investigation, Formal analysis, Conceptualization. **Lia Weiler:** Writing – original draft, Visualization, Formal analysis. **Johannes Haufe:** Writing – original draft, Visualization, Investigation, Formal analysis. **Anya Vollpracht:** Writing – review & editing, Supervision, Conceptualization.

Declaration of Competing Interest

The authors declare that they have no known competing financial interests or personal relationships that could have appeared to influence the work reported in this paper.

Data Availability

The data will be made available via electronic appendix

Acknowledgements

This work was partially funded by VGB PowerTech e.V.

Appendix A. Supporting information

Supplementary data associated with this article can be found in the online version at doi:10.1016/j.conbuildmat.2024.136151.

References

[1] M. Thomas, Supplementary Cementing Materials in Concrete, CRC Press, Boca Raton, 2013.
[2] B. Lothenbach, K. Scrivener, R. Hooton, Supplementary cementitious materials, Cem. Concr. Res. 41 (2011) 1244–1256, https://doi.org/10.1016/j.cemconres.2010.12.001.
[3] R. Snellings, K. Scrivener, Rapid screening tests for supplementary cementitious materials: past and future, Mater. Struct. (2015) 1–15, https://doi.org/10.1617/s11527-015-0718-z.
[4] F. Sybertz, Comparison of Different Methods for Testing the Pozzolanic Activity of Fly Ashes, in: V. Malhotra (Ed.), Fly Ash, Silica Fume, Slag, and Natural Pozzolans in Concrete, American Concrete Institute, Detroit, 1989, pp. 477–497.
[5] X. Li, R. Snellings, M. Antoni, N.M. Alderete, M. Ben Haha, S. Bishnoi, Ö. Cizer, M. Cyr, K. de Weerdt, Y. Dhandapani, J. Duchesne, J. Haufe, D. Hooton, M. Juenger, S. Kamali-Bernard, S. Kramar, M. Marroccoli, A.M. Joseph, A. Parashar, C. Patapy, J.L. Provis, S. Sabio, M. Santhanam, L. Steger, T. Sui, A. Telesca, A. Vollpracht, F. Vargas, B. Walkley, F. Winnefeld, G. Ye, M. Zajac, S. Zhang, K.L. Scrivener, Reactivity tests for supplementary cementitious materials: RILEM TC 267-TRM phase 1, Mater. Struct. 51 (2018) 136, https://doi.org/10.1617/s11527-018-1269-x.
[6] J. Chapelle, Attaque sulfo-calcique des laitiers et des pouzzolanes, Rev. Mat. éR. Constr. (1958) 136–145.
[7] F. Avet, R. Snellings, A. Alujas Diaz, M. Ben Haha, K. Scrivener, Development of a new rapid, relevant and reliable (R3) test method to evaluate the pozzolanic reactivity of calcined kaolinitic clays, Cem. Concr. Res. 85 (2016) 1–11, https://doi.org/10.1016/j.cemconres.2016.02.015.
[8] D. Londono-Zuluaga, A. Gholizadeh-Vayghan, F. Winnefeld, F. Avet, M. Ben Haha, S.A. Bernal, Ö. Cizer, M. Cyr, S. Dolenec, P. Durdzinski, L. Hanzic, J. Haufe, D. Hooton, S. Kamali-Bernard, X. Li, A.T.M. Marsh, M. Marroccoli, M. Mrak, Y. Muy, C. Patapy, M. Pedersen, S. Sabio, S. Schulze, R. Snellings, A. Telesca, A. Vollpracht, G. Ye, S. Zhang, K.L. Scrivener, Report of RILEM TC 267-TRM phase 3: Validation of the R3 reactivity test across a wide range of materials, Mater. Struct. 55 (2022) 142, https://doi.org/10.1617/s11527-022-01947-3.
[9] F. Avet, X. Li, M. Ben Haha, S.A. Bernal, S. Bishnoi, Ö. Cizer, M. Cyr, S. Dolenec, P. Durdzinski, J. Haufe, D. Hooton, M.C.G. Juenger, S. Kamali-Bernard, D. Londono-Zuluaga, A.T.M. Marsh, M. Marroccoli, M. Mrak, A. Parashar, C. Patapy, M. Pedersen, J.L. Provis, S. Sabio, S. Schulze, R. Snellings, A. Telesca, Michael Thomas, Felipe Vargas, A. Vollpracht, B. Walkley, F. Winnefeld, G. Ye, S. Zhang, K.L. Scrivener, Report of RILEM TC 267-TRM phase 2: optimization and testing of the robustness of the R3 reactivity tests for supplementary cementitious materials, Mater. Struct. 55 (2022) 92, https://doi.org/10.1617/s11527-022-01928-6.
[10] ASTM C1897-20 (2020) Standard Test Methods for Measuring the Reactivity of Supplementary Cementitious Materials by Isothermal Calorimetry and Bound Water. ASTM Int West Conshohocken, PA 1–5.
[11] H.S. Pietersen, A.L.A. Fraay, J.M. Bijen, Reactivity of fly ash at high pH, MRS Proc. 178 (1989) 377, https://doi.org/10.1557/PROC-178-139.
[12] A. Fernández-Jiménez, A. Palomo, Characterisation of fly ashes. Potential reactivity as alkaline cements, Fuel 82 (2003) 2259–2265, https://doi.org/10.1016/S0016-2361(03)00194-7.
[13] D. Glosser, A. Choudhary, O.B. Isgor, W.J. Weiss, Investigation of the reactivity of fly ash and its effect on mixture properties, Acids Mater. J. 116 (2019), https://doi.org/10.14359/51716722.
[14] Y.K. Cho, S.H. Jung, Y.C. Choi, Effects of chemical composition of fly ash on compressive strength of fly ash cement mortar, Constr. Build. Mater. 204 (2019) 255–264, https://doi.org/10.1016/j.conbuildmat.2019.01.208.
[15] D. Glosser, P. Suraneni, O.B. Isgor, W.J. Weiss, Estimating reaction kinetics of cementitious pastes containing fly ash, Cem. Concr. Compos. 112 (2020) 103655, https://doi.org/10.1016/j.cemconcomp.2020.103655.
[16] R. Snellings, Solution-controlled dissolution of supplementary cementitious material glasses at pH 13: the effect of solution composition on glass dissolution rates, J. Am. Ceram. Soc. 96 (2013) 2467–2475, https://doi.org/10.1111/jace.12480.
[17] OriginLab Corporation, OriginPro, Northampton, MA, USA.
[18] P. Schober, C. Boer, L.A. Schwarte, Correlation coefficients: appropriate use and interpretation, Anesth. Analg. 126 (2018) 1763–1768, https://doi.org/10.1213/ANE.0000000000002864.
[19] R.B. Finkelman, R.W. Stanton, Identification and significance of accessory minerals from a bituminous coal, Fuel 57 (1978) 763–768, https://doi.org/10.1016/0016-2361(78)90135-7.
[20] Y. Yudovich, M.P. Ketris, Chlorine in coal: a review, Int. J. Coal Geol. 67 (2006) 127–144, https://doi.org/10.1016/j.coal.2005.09.004.
[21] N. Montoya, F.J. Serrano, M.M. Reventós, J.M. Amigo, J. Alarcón, Effect of TiO2 on the mullite formation and mechanical properties of alumina porcelain, J. Eur. Ceram. Soc. 30 (2010) 839–846, https://doi.org/10.1016/j.jeurceramsoc.2009.10.009.
[22] C. Baudin, J.S. Moya, Influence of titanium dioxide on the sintering and microstructural evolution of mullite, J. Am. Ceram. Soc. 67 (1984) C-134–C-136.
[23] S. Lu, Physikalisch-chemische und mörteltechnische Untersuchungen zur Bewertung von Steinkohleflugaschen aus Kraftwerken. Dissertation, RWTH Aachen (1986).
[24] D. Manmohan, P.K. Mehta, Influence of pozzolanic, slag, and chemical admixtures on pore size distribution and permeability of hardened cement pastes, Cem. Concr. Aggr. 3 (1981) 63, https://doi.org/10.1520/CCA10203J.
[25] V.G. Papadakis, Effect of fly ash on Portland cement systems, Cem. Concr. Res. 29 (1999) 1727–1736, https://doi.org/10.1016/S0008-8846(99)00153-2.
[26] P. Chindaprasirt, C. Jaturapitakkul, T. Sinsiri, Effect of fly ash fineness on compressive strength and pore size of blended cement paste, Cem. Concr. Compos. 27 (2005) 425–428, https://doi.org/10.1016/j.cemconcomp.2004.07.003.

[27] S.H. Lee, H.J. Kim, E. Sakai, M. Daimon, Effect of particle size distribution of fly ash–cement system on the fluidity of cement pastes, Cem. Concr. Res. 33 (2003) 763–768, https://doi.org/10.1016/S0008-8846(02)01054-2.

[28] W.P. Linak, C.A. Miller, W.S. Seames, J.O. Wendt, T. Ishinomori, Y. Endo, S. Miyamae, On trimodal particle size distributions in fly ash from pulverized-coal combustion, Proc. Combust. Inst. 29 (2002) 441–447, https://doi.org/10.1016/S1540-7489(02)80058-X.

[29] F. Li, Q. Liu, M. Li, Y. Fang, Understanding fly-ash formation during fluidized-bed gasification of high-silicon-aluminum coal based on its characteristics, Energy 150 (2018) 142–152, https://doi.org/10.1016/j.energy.2018.02.137.

[30] E. Lang, Blastfurnace cements, in: J. Bensted, P. Barnes (Eds.), Structure and performance of cements, second. ed., Spon Press, London, 2002, pp. 310–325.

[31] C09 Committee, Specification for Coal Fly Ash and Raw or Calcined Natural Pozzolan for Use in Concrete, ASTM International, West Conshohocken, PA, 2019.

[32] J.E. Oh, Y. Jun, Y. Jeong, P.J. Monteiro, The importance of the network-modifying element content in fly ash as a simple measure to predict its strength potential for alkali-activation, Cem. Concr. Compos. 57 (2015) 44–54, https://doi.org/10.1016/j.cemconcomp.2014.12.001.

[33] T. Oey, J. Timmons, P. Stutzman, J.W. Bullard, M. Balonis, M. Bauchy, G. Sant, An improved basis for characterizing the suitability of fly ash as a cement replacement agent, J. Am. Ceram. Soc. 100 (2017) 4785–4800, https://doi.org/10.1111/jace.14974.

[34] R.A. Livingston, W. Bumrongjaroen, S. Essien, A.M. Amde, Application of Individual Glass Particle Data to Estimate Uncertainties in Bulk Fly Ash Chemical Compositions, in: D. Cong, D. Broton (Eds.), Advances in Cement Analysis and Concrete Petrography, ASTM International, 100 Barr Harbor Drive, PO Box C700, West Conshohocken, PA 19428-2959, 2019, pp. 41–54.

[35] H.J.H. Brouwers, R.J. van Eijk, Fly ash reactivity: Extension and application of a shrinking core model and thermodynamic approach, J. Mater. Sci. 37 (2002) 2129–2141, https://doi.org/10.1023/A:1015206305942.

[36] Y. Jin, W. Feng, D. Zheng, Z. Dong, H. Cui, Structure refinement of fly ash in connection with its reactivity in geopolymerization, Waste Manag 118 (2020) 350–359, https://doi.org/10.1016/j.wasman.2020.08.049.

[37] B.O. Mysen, D. Virgo, F.A. Seifert, The structure of silicate melts: Implications for chemical and physical properties of natural magma, Rev. Geophys. 20 (1982) 353, https://doi.org/10.1029/RG020i003p00353.

[38] P.T. Durdziński, R. Snellings, C.F. Dunant, M.B. Haha, K.L. Scrivener, Fly ash as an assemblage of model Ca–Mg–Na-aluminosilicate glasses, Cem. Concr. Res. 78 (2015) 263–272, https://doi.org/10.1016/j.cemconres.2015.08.005.

[39] J. Shekhovtsova, I. Zhernovsky, M. Kovtun, N. Kozhukhova, I. Zhernovskaya, E. Kearsley, Estimation of fly ash reactivity for use in alkali-activated cements - A step towards sustainable building material and waste utilization, J. Clean. Prod. 178 (2018) 22–33, https://doi.org/10.1016/j.jclepro.2017.12.270.

[40] P. Rapp, Effect of calcium chloride on portland cements and concretes, J. Res. Natl. Bur. Stand. 14 (1935).

[41] C. Shi, R.L. Day, Acceleration of the reactivity of fly ash by chemical activation, Cem. Concr. Res. 25 (1995) 15–21, https://doi.org/10.1016/0008-8846(94)00107-A.

[42] G. Giergiczny, Effect of some additives on the reactions in fly Ash-Ca(OH)2 system, J. Therm. Anal. Calorim. 76 (2004) 747–754.

[43] R.V. Venkateswara, Gnaneswar Kontham, Ramana Nelluru Venkata, S. Chundupalli, Effect of potassium chloride (KCl) on ordinary portland cement (OPC) concrete, Res. J. Chem. Sci. 1 (2011) 103–107.

[44] S. Deng, Y. Shu, S. Li, G. Tian, J. Huang, F. Zhang, Chemical forms of the fluorine, chlorine, oxygen and carbon in coal fly ash and their correlations with mercury retention, J. Hazard. Mater. 301 (2016) 400–406, https://doi.org/10.1016/j.jhazmat.2015.09.032.

[45] K. Schofield, The chemical nature of combustion deposition and corrosion: the case of alkali chlorides, Combust. Flame 159 (2012) 1987–1996, https://doi.org/10.1016/j.combustflame.2012.01.007.

[46] F. Zhu, M. Takaoka, K. Shiota, K. Oshita, Y. Kitajima, Chloride chemical form in various types of fly ash, Environ. Sci. Technol. 42 (2008) 3932–3937, https://doi.org/10.1021/es7031168.